PHYSICAL REVIEW B **81**, 020404(R) (2010)

Control of chirality normal to the interface of hexagonal magnetic and nonmagnetic layers

Jason T. Haraldsen and Randy S. Fishman
Materials Science and Technology Division, Oak Ridge National Laboratory, Oak Ridge, Tennessee 37831, USA
(Received 2 November 2009; revised manuscript received 11 December 2009; published 8 January 2010)

We study the net chirality created by the Dzyaloshinskii-Moriya interaction (DMI) at the boundary between hexagonal layers of magnetic and nonmagnetic materials. It is shown that another mechanism besides elastic torsion is required to understand the change in chirality observed in Dy/Y multilayers during field cooling. This Rapid Communication demonstrates that, due to the overlap between magnetic and nonmagnetic atoms, interfacial steps may produce a DMI normal to the interface in magnetic heterostructures.

DOI: 10.1103/PhysRevB.81.020404 PACS number(s): 75.70.Cn, 61.05.fg, 75.10.−b, 75.30.Gw

Chiral magnetic ordering is produced by the competition between ferromagnetic and antiferromagnetic interactions and plays an important role in nanomagnetism within complex systems such as spin glasses and other noncollinear magnetic structures.[1–4] While chirality can be observed in many noncollinear systems, it is most widely studied in helical or cycloidal magnetic structures.[5–8] The ability to experimentally control chirality remains an active area of research and advances have been made in the overall detection of chirality by techniques like polarized neutron scattering.[5–13] However, the mechanisms that produce chirality continue to challenge our theoretical understanding.

In a system without broken inversion symmetry, the net chirality throughout a material is zero, giving equal weight to left- and right-handed domains.[3] When inversion symmetry is broken, a Dzyaloshinskii-Moriya interaction (DMI) may favor one handedness over another,[14–18] thereby inducing a net chirality. A DMI is the driving force behind the net chirality observed in many magnetic structures.[8–11]

One way to obtain a net chirality is through elastic torsion deformation, whereby an elastic lattice distortion with left or right handedness produces an excess population of left- or right-handed chiral domains.[6,8] Fedorov *et al.* studied the phenomenological origin of the DMI created by the elastic torsion in annealed Ho filings.[6] Detailed experimental measurements of $CsMnBr_3$ and bulk Ho using polarized neutron scattering examined the critical behavior of the chiral order produced by torsion.[12,13] For $ZnCr_2Se_4$, chirality can be controlled by using crossed electric and magnetic fields.[19,20]

In 2008, Grigoriev *et al.* observed a net chirality in Dy/Y multilayers.[10] As in many other rare-earth systems,[21] the Dy spin moments are aligned in plane with the helical wave vector propagating in the z direction. So the chirality of the helix is normal to the multilayer interface. Grigoriev *et al.* showed that the net chirality can be changed by applying a magnetic field during cooling [field cooling (FC)].[10] Since elastic torsion is a macroscopic mechanical deformation of the entire system, zero-field-cooled (ZFC) and FC samples should have the same net chirality. However, as the strength of the field increased, the overall handedness of the system changed sign.[10] This revealed that some other mechanism must compete with torsion to control chirality.

Recent experiments have examined the relationship between multilayer and domain interfaces and the existence of a net in-plane chirality for various square lattices.[10,11] By breaking inversion symmetry, the presence of an interface or surface may produce a DMI that favors a specific chirality.[11] In this Rapid Communication, we examine the nature of the DMI induced at the interfaces between hexagonal layers of magnetic and nonmagnetic materials. While a smooth or flat interface cannot produce a normal DM vector, the introduction of defects and steps at the interface can produce a net normal chirality in hexagonal systems.

The general DMI energy is given by

$$H_{\mathrm{DM}} = \sum_{i \neq j} \mathbf{D}_{ij} \cdot [\mathbf{S}_i \times \mathbf{S}_j], \tag{1}$$

where $\mathbf{S}_i$ is the spin at site i and $\mathbf{D}_{ij}$ is the interaction vector between sites i and j.[14–18] Typically, D_{ij} is of order $0.1J$,[16,17] where J is the isotropic coupling. The chirality $\mathbf{C}_{ij}=[\mathbf{S}_i \times \mathbf{S}_j]$ determines the clockwise or counterclockwise nature of the magnetic order.[8] To minimize the energy and maximize the DMI contribution, $\mathbf{D}_{ij}$ and $\mathbf{C}_{ij}$ must be antiparallel.

Since the DMI only appears when inversion symmetry is violated, it is important to understand how the lattice affects the overall chirality. At an interface between magnetic and nonmagnetic layers, Levy and Fert[22] established that the interaction between two magnetic sites at $\mathbf{R}_i$ and $\mathbf{R}_j$ with neighboring nonmagnetic sites at $\mathbf{R}_n$ produces the DM vector

$$\mathbf{D}_{ij} = \frac{D_0}{R_{ij}} \sum_n \frac{\mathbf{R}_{in} \cdot \mathbf{R}_{jn} (\mathbf{R}_{in} \times \mathbf{R}_{jn})}{(R_{in} R_{jn})^3}, \tag{2}$$

where D_0 is proportional to the spin-orbit coupling and $\mathbf{R}_{in} = \mathbf{R}_i - \mathbf{R}_n$ is the vector connecting magnetic site (i) to the nonmagnetic site (n).[3,22]

Specializing to the hexagonal lattice (shown in Fig. 1) and using the general rules and guidelines provided by Dzyaloshinskii[14,15] and Moriya,[16,17] a smooth interface will have $\mathbf{D}_{ij}$ pointing in the xy plane. Figure 1 illustrates the packing of hexagonal-closed-packed (HCP) [Fig. 1(a)] and face-centered-cubic (FCC) [Fig. 1(b)] lattices, where a is the lattice spacing within each plane and $c/2$ is the separation between adjacent planes. The in-plane $\mathbf{D}_{ij}$ vectors are shown in Fig. 1(c) and their magnitudes for HCP and FCC configurations are

$$|\mathbf{D}_{ij}|_{\mathrm{HCP}} = \frac{12\sqrt{3} D_0 (\gamma + 2\sqrt{1+\gamma^2})}{a^3 \sqrt{1+\gamma^2} (4+3\gamma^2)^2},$$

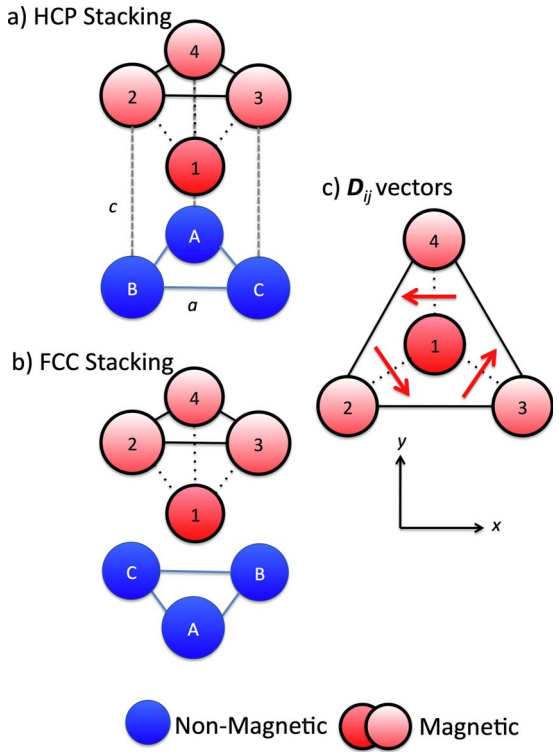

FIG. 1. (Color online) (a) HCP stacking with nonmagnetic (A–C) and magnetic (1–4) sites. (b) FCC stacking with same nonmagnetic and magnetic sites. (c) The in-plane $\mathbf{D}_{ij}$ vectors created between magnetic site 1 and sites 2–4 for both HCP and FCC lattices.

$$|\mathbf{D}_{ij}|_{\mathrm{FCC}} = \frac{108\gamma D_0}{a^3\sqrt{1+3\gamma^2}(4+3\gamma^2)^2}, \tag{3}$$

with $\gamma = c/a$. Since a smooth interface has $\mathbf{D}_{ij}$ in plane, the DMI will not contribute to the normal chirality of the system ($\mathbf{D}_{ij}$ is perpendicular to $\mathbf{C}$, not parallel). It should also be noted that the sum of the $\mathbf{D}_{ij}$ vectors around any site i is zero. For ferromagnetic order in each plane, no net DMI is produced by the interface. Thus, interfacial defects may be required to explain the presence of normal chirality.

It is well established that the energy of an interface between magnetic and nonmagnetic layers is lowered by the creation of defects and steps.[23–26] If defects or steps are present, then it may be possible to create a net nonzero component D^z_{net} normal to the interface. In Fig. 2(a), the nonmagnetic (blue circles without borders) sites have a stepped interface with no overlap between the magnetic (red circles with solid dark borders) sites and the nonmagnetic material. Figures 2(b)–2(d) show some possibilities for interface overlap with different interface angles Θ. Overlap occurs when one or more of the covering sites (2–4 in Fig. 1) are nonmagnetic. The black square and triangle in Fig. 2(a) illustrate the different possible stacking mechanisms.[27] Whereas the HCP lattice orders in an alternating square/triangle stacking pattern, the FCC lattice orders in a square/square or triangle/triangle stacking pattern. While this Rapid Communication focuses on the HCP stacking, our results can also be applied to the FCC lattice by rotating the appropriate layers.

While Fig. 3(a) shows the possible adjacent step positions

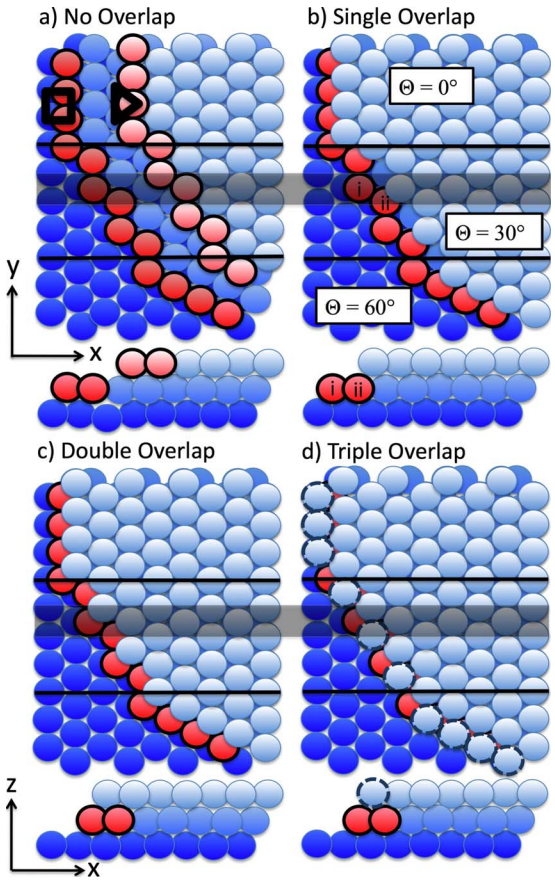

FIG. 2. (Color online) The HCP stacking of nonmagnetic (blue/light gray without borders) and magnetic (red/gray with solid dark borders) sites for interface angles $\Theta = 0°$, 30°, and 60° with (a) zero, (b) single, (c) double, and (d) triple overlapping of steps. The larger upper panels show the xy plane while the smaller lower panels represent the z axis projection along the shaded region. The lighter shades of color show an increase in layer (as illustrated under each panel), while the black square and triangle show the different stacking mechanisms. Single, double, and triple refer to the site with the maximum amount of overlap. Note that (c) and (d) differ by extra nonmagnetic sites (blue/light gray with dashed light borders).

P_k, Figs. 3(b)–3(d) illustrate the various overlap configurations. Each step site P_k produces an individual $\mathbf{D}_{P_k}$ between site 1 and the magnetic sites in the layer above. Note that $\mathbf{D}_{P_k} = \Sigma_m \mathbf{D}^{P_k}_{1m}$, where m denotes the magnetic sites present (2, 3, and/or 4.) These values are given in Table I. Depending on which sites adjacent to site 1 are nonmagnetic, the net DM vector is

$$\mathbf{D}_{net} = \sum_k \mathbf{D}_{P_k}. \tag{4}$$

Assuming $\gamma = \sqrt{8/3}$ (ideal stacking), Fig. 3 and Table I give the components for D^z_{net} produced by all adjacent sites depending on the amount of overlap. All D^z_{net} values for any site configuration can be determined through rotations of the systems shown in Fig. 3.

In Fig. 4(a), $D^z_{net}a^3/D_0$ is plotted as a function of the lattice ratio γ for the different adjacent positions for the single (dark blue lines) and double (light green lines) overlap cases shown in Figs. 2(b) and 2(c). We find that the separa-

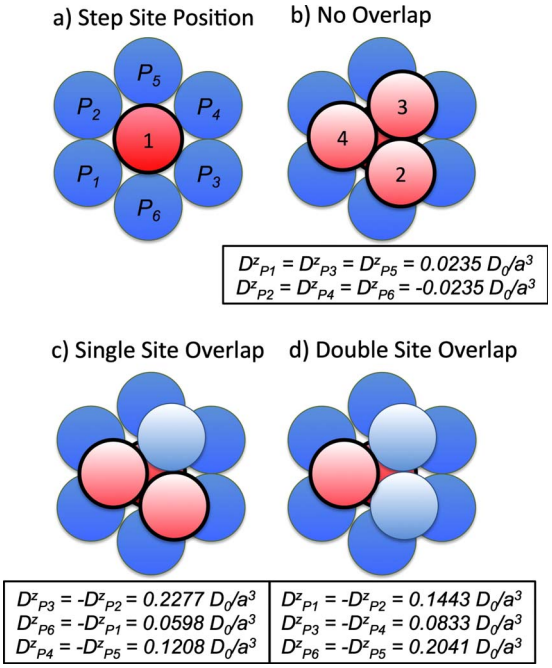

FIG. 3. (Color online) (a) The site position labels P_k for adjacent nonmagnetic sites in contact with magnetic site 1. The total $D^z_{P_k}$ contribution with (b) no overlap, (c) single site overlap, and (d) double site overlap is given for each adjacent site P_k. Here, $\gamma = \sqrt{8/3}$ and the numbers 2–4 correspond to the magnetic sites in Fig. 1.

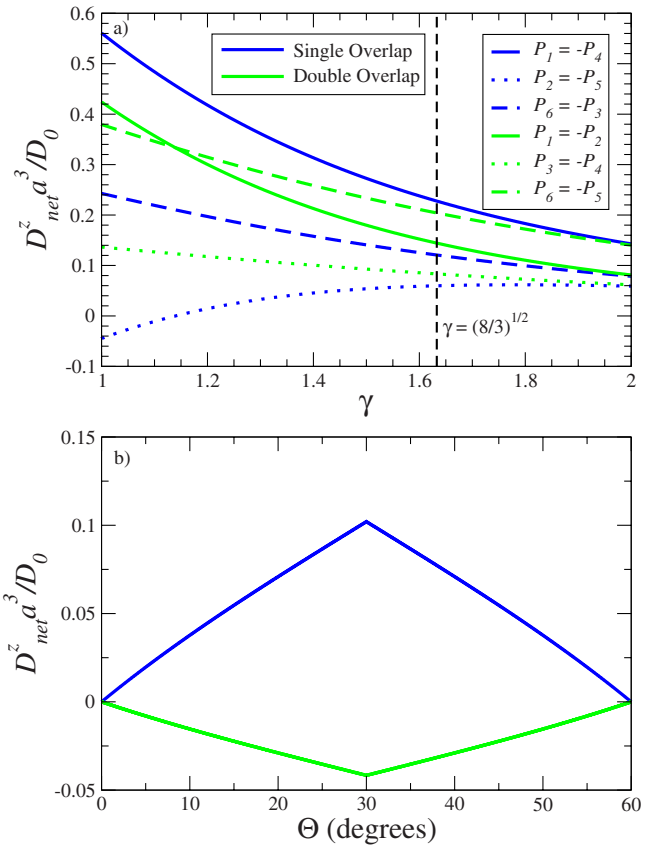

FIG. 4. (Color online) (a) $D^z_{net}a^3/D_0$ for the specific adjacent step positions as a function of the ratio γ. Here, the dark blue/dark gray lines represent the single overlap case and the light green/light gray lines represent the double overlap case. (b) $D^z_{net}a^3/D_0$ as a function of the interface angle Θ for both single and double overlap cases. These plots are for the HCP lattice with square-type steps.

tion between layers can dramatically changes the on-site DMI. Consequently, multilayers that exhibit a significant magnetostriction should exhibit a distinct change in the DMI with increasing magnetic field. It is may also be possible to change the net chirality through pressure or strain.

Interfaces with no overlap produce no D^z_{net} component due to the cancellation of positive and negative DMIs. On the contrary, when site overlap exists [as in Figs. 2(b)–2(d)], the interface can create a nonzero D^z_{net} component. This value will vary with the interface angle Θ as shown in Fig. 4(b). Notice that $|D^z_{net}|$ reaches a maximum at $\Theta = 30°$ and vanishes for perfect steps with $\Theta = 60°$. These values were

TABLE I. The z component of $\mathbf{D}^{P_k}_{ij}a^3/D_0$ for the no overlap and single overlap cases. Double overlap case is given in Fig. 3 for $D^{P_k}_{14}$. Since all other sites are nonmagnetic, their values are zero. All values are to be multiplied by D_0/a^3.

No overlap case						
$D^{P_k}_{1j}$	P_1	P_2	P_3	P_4	P_5	P_6
$D^{P_k}_{12}$	−0.2041	−0.0833	0.1443	0.2041	0.0833	−0.1443
$D^{P_k}_{13}$	0.0833	0.2041	−0.2041	−0.1443	0.1443	−0.0833
$D^{P_k}_{14}$	0.1443	−0.1443	0.0833	−0.0833	−0.2041	0.2041
$D^z_{P_k}$	0.0235	−0.0235	0.0235	−0.0235	0.0235	−0.0235
Single overlap case[a]						
$D^{P_k}_{1j}$	P_1	P_2	P_3	P_4	P_5	P_6
$D^{P_k}_{12}$	−0.0598	0.0610	0.2887	0.3485	0.2277	0
$D^{P_k}_{14}$	0	−0.2887	−0.0610	−0.2277	−0.3485	0.0598
$D^z_{P_k}$	−0.0598	−0.2277	0.2277	0.1208	−0.1208	0.0598

[a]$D^{P_k}_{13}$ is zero due to site 3 being nonmagnetic in this case.

determined by averaging magnetic sites i and ii shown in Fig. 2 for the single and double overlap cases. As shown in Fig. 4(b), the addition of an extra overlap site dramatically changes the D_{net}^{z} component and effectively flips the chirality.

While these defects are local, the chirality of the whole system is affected due to the in-plane ferromagnetic coupling, such as that present in rare-earth multilayers. The normal DMI induced by defects may play a particularly important role for the field-induced chirality observed by Grigoriev *et al.* in Dy/Y multilayers.[10] For the multilayers studied in Ref. 10, the interfaces have an incline angle ϕ of about 5° between the normal to the layer and the crystallographic c axis. Therefore, the multilayer interface has at least one step per every ten sites. Using the methods described above with $a=3.5$ Å, the maximum D_{net}^{z} is about $0.002D_0$ per magnetic site at the interface.

Recent scanning tunneling microscopy measurements have shown that interfaces in multilayers are typically of a ridged and rough nature with an asymmetry between A/B and B/A interfaces.[28] The roughness of the interface may help us to explain the presence of a DMI in some multilayer materials due to the increased possibility of overlap. An asymmetry between the Dy/Y and Y/Dy interfaces is required to explain the net DMI. This effect can be studied by synthesizing multilayer materials with systematic steps and defects. A series of multilayers that are grown with different incline angles or interface angles should show a systematic change in the net chirality.

The DMI produced by interfacial defects is likely to be affected by increasing the magnetic field in the FC process due to the increase in the magnetic correlation length in the plane. Since the correlation length in the ZFC system is less than that of the FC system, the number of defect-induced chiral sites will overcome or augment any chirality produced by elastic torsion at zero field. With increasing field applied during cooling, the spin helix will engulf a greater number of defect sites. This will in turn change the overall DMI since it is determined by a sum over the affected sites. Neutron-scattering measurements should be able to verify the change in the in-plane correlation length with field.

In conclusion, we present a mechanism for the creation of the DMI, which incorporates interfacial defects and steps to produce interaction vectors normal to the interface. We provide a straightforward method for calculating and estimating the interaction vectors for any step configuration. We show that defects are critical to creating a DMI and that lattice changes along with defects can have a dramatic effect on chirality. While these are local defects, an in-plane ferromagnetic coupling will help propagate the chirality throughout the system. It is expected that these calculations will help in the overall understanding of the DMI within multilayers and chirality in general. The ability to control the DMI at interfaces may lead to the design of new materials that have helical or cycloidal structures with net chirality.

We would like to acknowledge useful discussions with Z. Zhang. This research was sponsored by the Laboratory Directed Research and Development Program of Oak Ridge National Laboratory, managed by UT-Battelle, LLC for the U.S. Department of Energy under Contract No. DE-AC05-00OR22725 and by the Division of Materials Science and Engineering and the Division of Scientific User Facilities of the U.S. DOE.

[1] D. A. Smith, J. Magn. Magn. Mater. **1**, 214 (1976).
[2] A. Fert and P. M. Levy, Phys. Rev. Lett. **44**, 1538 (1980).
[3] A. Crépieux and C. Lacroix, J. Magn. Magn. Mater. **182**, 341 (1998).
[4] K. Kimura, H. Nakamura, K. Ohgushi, and T. Kimura, Phys. Rev. B **78**, 140401(R) (2008).
[5] G. Shirane, R. Cowley, C. Majkrzak, J. B. Sokoloff, B. Pagonis, C. H. Perry, and Y. Ishikawa, Phys. Rev. B **28**, 6251 (1983).
[6] V. I. Fedorov, A. G. Gukasov, V. Kozlov, S. V. Maleyev, V. P. Plakhty, and I. A. Zobkalo, Phys. Lett. A **224**, 372 (1997).
[7] D. N. Aristov and S. V. Maleyev, Phys. Rev. B **62**, R751 (2000).
[8] S. V. Maleyev, Physica B **297**, 67 (2001).
[9] S. V. Grigor'ev, A. I Okorokov, Yu. O. Chetverikov, D. Yu. Chernyshev, H. Eckerlebe, K. Pranzas, and A. Schreyer, JETP Lett. **83**, 478 (2006).
[10] S. V. Grigoriev, Yu. O. Chetverikov, D. Lott, and A. Schreyer, Phys. Rev. Lett. **100**, 197203 (2008).
[11] M. Bode, M. Heide, K. von Bergmann, P. Ferriani, S. Heinze, G. Bihlmayer, A. Kubetzka, O. Pietzsch, S. Blügel, and R. Wiesendanger, Nature (London) **447**, 190 (2007).
[12] V. P. Plakhty, W. Schweika, Th. Brückel, J. Kulda, S. V. Gavrilov, L.-P. Regnault, and D. Visser, Phys. Rev. B **64**, 100402(R) (2001).
[13] V. P. Plakhty, J. Kulda, D. Visser, E. V. Moskvin, and J. Wosnitza, Phys. Rev. Lett. **85**, 3942 (2000).
[14] I. Dzyaloshinskii, Sov. Phys. JETP **5**, 1259 (1957).
[15] I. Dzyaloshinsky, J. Phys. Chem. Solids **4**, 241 (1958).
[16] T. Moriya, Phys. Rev. Lett. **4**, 228 (1960).
[17] T. Moriya, Phys. Rev. **120**, 91 (1960).
[18] P. W. Anderson, Phys. Rev. **115**, 2 (1959).
[19] K. Siratori, J. Akimitsu, E. Kita, and M. Nishi, J. Phys. Soc. Jpn. **48**, 1111 (1980).
[20] M. L. Plumer, H. Kawamura, and A. Caille, Phys. Rev. B **43**, 13786 (1991).
[21] R. J. Elliot, *Magnetic Properties of Rare Earth Metals* (Plenum Publishing Company, New York, 1972).
[22] P. M. Levy and A. Fert, Phys. Rev. B **23**, 4667 (1981).
[23] Y. Mo, K. Varga, E. Kaxiras, and Z. Zhang, Phys. Rev. Lett. **94**, 155503 (2005).
[24] Y. Mo, W. Zhu, E. Kaxiras, and Z. Zhang, Phys. Rev. Lett. **101**, 216101 (2008).
[25] J. Shen, R. Skomski, M. Klaua, H. Jenniches, S. S. Manoharan, and J. Kirschner, Phys. Rev. B **56**, 2340 (1997).
[26] P. Gambardella, A. Dallmeyer, K. Maiti, M. C. Malagoli, W. Eberhardt, K. Kern, and C. Carbone, Nature (London) **416**, 301 (2002).
[27] Y. Girard, G. Baudot, V. Repain, S. Rohart, S. Rousset, A. Coati, and Y. Garreau, Phys. Rev. B **72**, 155434 (2005).
[28] S. J. May, A. B. Shah, S. G. E. te Velthuis, M. R. Fitzsimmons, J. M. Zuo, X. Zhai, J. N. Eckstein, S. D. Bader, and A. Bhattacharya, Phys. Rev. B **77**, 174409 (2008).